Direct mapping of microscopic polarization in ferroelectric $x(BiScO_3)$-$(1-x)(PbTiO_3)$ throughout its morphotropic phase boundary

K. Datta*
Department of Crystallography and Structural Physics, Friedrich-Alexander-Universität Erlangen-Nurnberg, Staudtstraße 3, Erlangen 91058, Germany
and Department of Earth Sciences, Universität Hamburg, Hamburg 20146, Germany

A. Richter and M. Göbbels
Department of Minerologie, Friedrich-Alexander-Universität Erlangen-Nürnberg, Schlossgarten 5a, Erlangen 91054, Germany

D. A. Keen
ISIS Facility, Rutherford Appleton Laboratory, Harwell Oxford, Didcot OX11 0QX, United Kingdom

R. B. Neder
Department of Crystallography and Structure Physics, Friedrich-Alexander-Universität Erlangen-Nürnberg, Staudtstraße 3, Erlangen 91058, Germany

(Received 26 June 2015; revised manuscript received 23 September 2015; published 3 February 2016)

Pair distribution functions of ferroelectric xBiScO$_3$-$(1-x)$PbTiO$_3$, obtained from neutron total scattering data, were examined and modeled utilizing the reverse Monte Carlo technique to depict exclusively the local structure of this compound throughout its reported morphotropic phase boundary (MPB). Microscopic polarizations due to the cation shifts have been mapped out from the refined crystal structure as a function of composition in order to reveal individual cation behavior driven by the composition. Direct evidences are provided for large static displacements of the cations ($\sim 0.2-0.5$ Å), local cation ordering between Ti and Sc, and a categorical change of favored polarization directions of the cations at the conjuncture of the MPB. Apart from Sc, all cations have demonstrated an apparent transition from a relatively defined directional distribution to a broad and random distribution at $x = x_{MPB}$, suggesting a flattening of the local potential function for them. These features can further be correlated with the general concept of structural instability of a ferroelectric system at the MPB, which is often linked to the manifestation of enhanced physical properties.

DOI: 10.1103/PhysRevB.93.064102

Structural phase transitions driven by composition have become a riveting aspect in the field of ferroelectric and piezoelectric materials since the revelation of an emphatic connection between the structure and the property in the case of lead zirconium titanate ($PbZr_xTi_{1-x}O_3$) [1], commonly known as PZT. In particular, a point in the phase diagram, depicted ordinarily as a transition point from tetragonal to rhombohedral lattice symmetry, was called morphotropic phase boundary (MPB) where materials often exhibit enhanced physical properties. Driven by this concept of either generating a structural instability between two or several different phases or to find a sandwiched monoclinic phase as in PZT [2] by carefully tweaking the composition, there have been an extensive range of structural reports on a broad range of systems in order to manufacture novel systems with improved qualities. In 2001, Eitel *et al.* first published a list of binary solid solutions based on perovskite structure-type (ABO_3), especially suitable for high temperature piezoelectric applications. Among them xBiScO$_3$-$(1-x)$PbTiO$_3$ (xBS $-$ PT) showed excellent physical properties for a wide range of temperature (at $x = 0.36$, $T_c = 723$ K, $d_{33} = 460$ pC/N, $k_p = 0.56$, and $K_{33}^T = 2010$) in comparison with the industrial standard PZT [3,4]. A detailed phase diagram of this system was first reported in 2004 [5] combining temperature dependent TEM, dielectric, and calorimetry data, which showed the existence of the tetragonal-rhombohedral MPB at $x = 0.36$. Since then there have been several structural reports to elucidate the MPB [6,7], primarily suggesting the presence of a low-symmetry monoclinic phase (space group Cm) along with the other phases. In general, accurate determination of different phases through the average or long-range structural analysis, such as Rietveld refinements of powder diffraction data, is challenging for complex ferroelectric solid solutions, which often consist of short-range chemical ordering, large static disorder, defects, and structural inhomogeneity [8]. For example, ambiguity still exists in determination of the best refinement solution of xBS $-$ PT at $x \approx x_{MPB}$ as different combinations of phases giving similar values of agreement factor, and for $x > x_{MPB}$ subtle features were observed which are better modeled by a single monoclinic phase instead of a rhombohedral phase [7,9]. In addition a few recent reports [9–11] which showed that with the application of either electric field or stress it is possible to induce irreversible structural transformations around the MPB composition further indicates that mere average structural models which assume uncorrelated motions of the cations are insufficient to establish detailed structure-property relationships. Evidence for nonperiodic features inconsistent with the average symmetry of the structures, such as large local cation shifts, have already been pointed out by

*kaustuv.datta@uni-hamburg.de

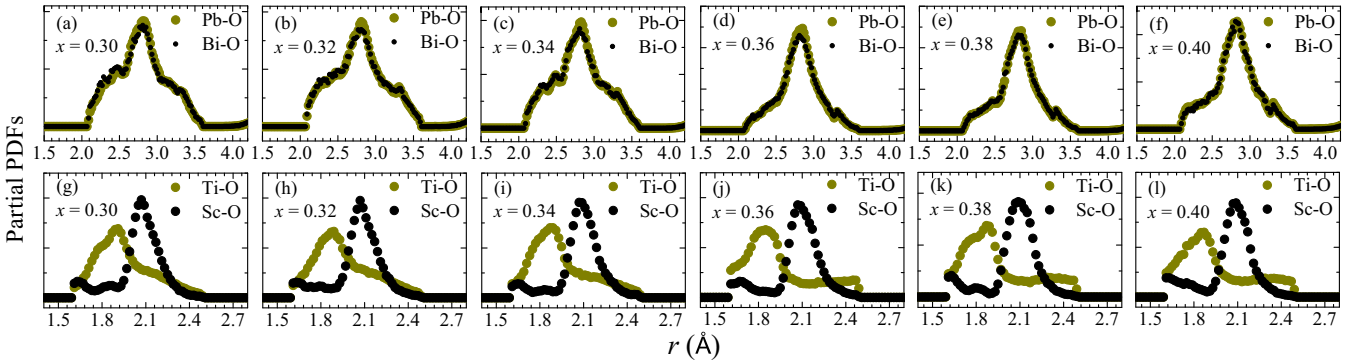

FIG. 1. Partial PDFs, averaged over ten independent RMC runs, of the metal-oxygen pairs obtained from the RMC calculations as a function of composition.

several reports on Pb-based ferroelectric systems for which strong diffuse scattering was observed [12,13]. Therefore, investigation and understanding of the structure at the very atomic level to depict cation displacements and their local environment are crucial for mixed-ion complex ferroelectric systems as local distortions, correlated shifts, and ordering can heavily influence their properties [14–16].

In this context, the total scattering method where pair distribution functions (PDF) are obtained from the Fourier transformation of the normalized and corrected diffraction intensity is a powerful technique to reveal the local structural information [17]. The PDF, which can simply be thought of as a histogram of interatomic separations in a material, provides a lot of intuitive information about the nearest neighbor distances and their distributions even before any analysis. Further structural details can be extracted from model-based refinements, especially through reverse Monte Carlo (RMC) simulations [18,19]. The PDF method has already been applied to a number of complex ferroelectric materials, such as PZT [20], $Pb(Mg_{1/3}Nb_{2/3})O_3$ (PMN) [21], $Pb(Sc_{1/2}Ta_{1/2})O_3$ (PST) [22], and $Pb(Zn_{1/2}Nb_{1/2})O_3$-$x$$PbTiO_3$ (PZN-PT) [23], including some lead-free systems like $Ba(Ti_xZr_{1-x})O_3$ [24] and $Na_{1/2}Bi_{1/2}TiO_3$ [25], which have provided new insights for a better understanding of the structure-property relationships.

In this paper we focus on the specifics of the local environment of each cation including their shifts and ordering within the range of the first few neighbors in order to fingerprint their role in structural phase transition driven by the composition. In particular, to quantify our observations we adopted the model-based refinement against the neutron PDF data through RMC technique, which allows one to refine a plausible model consisting of a large number of atoms ($\sim$10 000) against the experimental data by moving them in a complete random fashion. In doing so, it is possible to evaluate many aspects of the local structure, at least statistically, such as correlated atomic displacements, chemical short-range order, and the evolution of local structural characteristics of the system upon doping. Here we have focused on elucidating the local environment of each cation through assessing their displacements and displacement directions relative to their oxygen environment. For ferroelectric systems, in general, the knowledge of local shifts of the cations is crucial in order to understand the structure-property relationships since the ensuing local polarization drives both the structure and the physical properties of the system.

Powder samples of xBS $-$ PT with varying composition were prepared following the conventional solid state synthesis route where starting materials were oxides of individual cations, and the compositions were later verified by the electron microprobe analysis [26]. Neutron total scattering data were collected at the GEM diffractometer of the ISIS facility in UK. Further data processing in order to obtain the PDFs were done using the GUDRUN package. Data modeling as a function of composition based on the RMC method was carried out in RMCProfile software [27]. The starting model for the RMC runs consisting of $14 \times 14 \times 14$ tetragonal (space group $P4mm$) unit cells was adopted from an earlier report based on Rietveld refinements [7]. All structural analyses of the refined models were carried out using DISCUS package [28].

The partial PDFs (bond length distributions) for the metal-oxygen correlations obtained from the RMC calculations for different compositions have been shown in Fig. 1 within the range of first neighbor distances. It is evident that there is hardly any difference between Pb-O and Bi-O histograms, suggesting that the Pb and the Bi are having very similar oxygen environment and distribution of local shifts irrespective of the composition. Although with the presence of the $6s^2$ lone-pair electrons Bi is anticipated to follow Pb in terms of local distortions, it should also be noted that Pb and Bi have very similar neutron scattering lengths (9.405 fm and 8.532 fm, respectively). Therefore, the data may not distinguish Pb and Bi distinctly. The Pb/Bi-O histograms could be assigned to three main distances at around 2.3, 2.8, and 3.2 Å for $x \leqslant 0.34$. However, for $x \geqslant 0.36$, the Pb/Bi-O histograms are nearly symmetric single peaks centered at 2.8 Å. The diminished humps around 2.3 and 3.2 suggest that a significant fraction of the A-site cations have moved into a more symmetric position with respect to its 12 oxygen neighbors (Fig. 2), and hence most A-site cations have relatively isotropic oxygen environment for compositions $x \geqslant x_{\mathrm{MPB}}$. It is also apparent that the A-O correlations do not have significant differences among the compositions for $x \leqslant 0.34$ and for $x \geqslant 0.36$; however, the development is rather sharp from $x = 0.34$ to 0.36. This provides crucial information on the mechanism of the structural phase transition observed as a function of composition. The characteristics of A-O histograms strongly suggest that the changes in the average

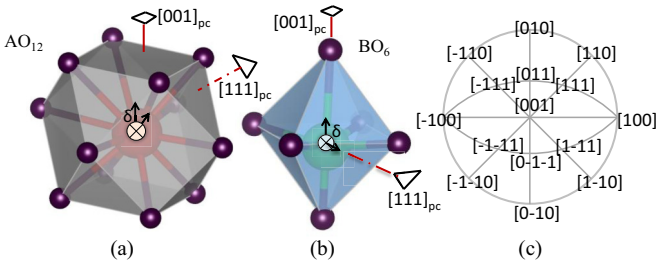

FIG. 2. Oxygen environment for (a) A-site cations and (b) B-site cations of a perovskite structure-type (ABO_3) with the fourfold and the threefold axis along the [001] and the [111] pseudocubic axis, repectively. (c) The stereographic projection of a cubic crystal looking along the [001] direction.

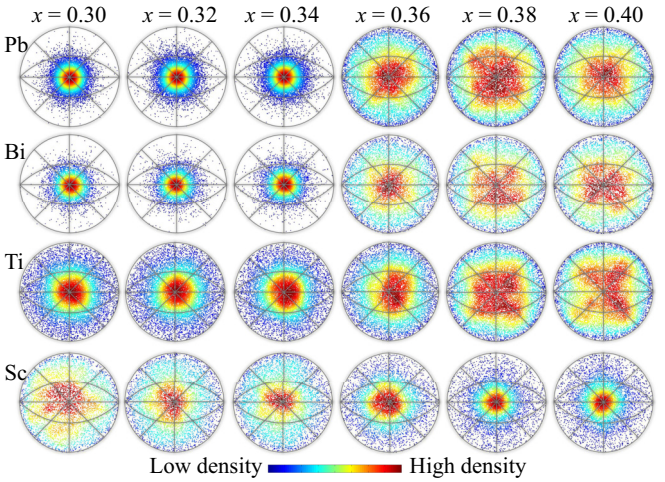

FIG. 3. [001] stereographic projections of the cation shifts from the center of their oxygen polyhedra.

structure around the MPB composition are correlated with a sharp and distinguishable local displacement of the A-site cations instigated by the doping. This further corroborates the Raman scattering data collected on the same batch of samples [26], which suggested the A-cation phonon mode around 60 cm^{-1} is strongly affected at the onset of the MPB.

Contrary to the A-site cations, B-site cations behave quite distinctly since there are less obvious changes in the B-O histograms as a function of composition to follow the average structural evolution or to track down the MPB. However, it is evident that Ti and Sc have very different average position with respect to their oxygen octahedra. The main population of Ti-O distances peaks around 1.8–1.9 Å with an extended hump around 2.2 Å, which is further flattened for compositions $x \geqslant 0.36$. The asymmetric peak shapes indicate an anisotropic oxygen environment for Ti throughout the studied range of composition in comparison to Sc, for which the histograms peak more symmetrically and consistently around 2.1 Å.

For a detailed quantitative analysis of the displacements of the cations, we followed a similar method recently reported for ferroelectric systems like $Na_{0.5}Bi_{0.5}TiO_3$ [25] and PZT [20]. The aim of this method is to calculate the displacement vector of a cation from the center of its oxygen polyhedron (Fig. 2) and then to project that in a stereographic map in order to extract a statistical description of the directions of the shifts. Figure 3 illustrates such plots for different compositions showing the distribution of the shift directions of the cations as determined from the center of the BO_6 and AO_{12}. The color of the points in the plots has been assigned following the density distribution around that particular point to depict the trend of the direction of the shifts. It is evident that, for $x < 0.36$, A-site cations have a sharp distribution of the shift directions centered at [001]; however, for $x \geqslant 0.36$ the distributions have become very broad with flat density maximums around [001]. The loss of apparent sharp symmetric density distributions for $x \geqslant 0.36$ provides a direct evidence for an abrupt change in the behavior of the A-site cations at the conjuncture of the MPB. As a whole, this relates to a situation where either of the A-site cations are moving from a unidirectional local polarization to a randomly oriented local polarization driven by the composition. The coupled behavior of Pb and Bi ions, as mentioned before, is possibly a consequence of the poor contrast between them in neutron scattering data. On the other hand, the B-site cations behave distinctively from each other. For $x < 0.36$ the Ti ions have mostly [001] polarization including a bit of broadness in the distribution; however, it undergoes similar transformation like Pb for $x \geqslant 0.36$. But unlike Pb, Ti provides a trend for the composition $x = 0.40$ where the maximum density is lining along the trace of (1-10) and (110) planes. The direction distribution for Sc ions is highly scattered for $x = 0.30$; however, gradually with increasing concentration, it has condensed into a sharp and symmetric distribution centered at [001], which is primarily due to the size constraint.

Generally speaking, Fig. 3 depicts the evolution of the microscopic polarization in the system as a function of composition from which one can conceive of the local ordering of the cations that can be further linked to the local and the average symmetry of the system. For example, the shifts of the A-site cations strongly favors the tetragonal distortion until x reaches to 0.36 and after that, it does not exclusively suggest a single specific symmetry, rather it is indicative of a mixture of different symmetry distortions. The Ti distortions can be thought of as weakly coupled to the A-site cations, initially maintaining a tetragonal distortion, although it has evolved to a monoclinic distortion (categorically as a M_A type monoclinic distortion [20]) through a region of mixed symmetry distortions. A-site cation polarization directions are consistent with the average symmetry of the system where the powder diffraction patterns for compositions $x < 0.36$ have been modeled with a single tetragonal phase and the MPB compositions 0.36–0.37 were modeled with more than one phase [6,7,29]. However, at $x = 0.40$, the material has been reported to be modeled equally well with a single phase of either rhombohedral space group $R3m$ or monoclinic space group Cm [7,9]. Therefore, although the A-site cation local polarization does not strictly follow the predicted average symmetry for $x = 0.40$, the local polarization of Ti ions reflects more of the average monoclinic symmetry. The coupled characteristics between the A-site and the B-site cations for compositions $x < x_{MPB}$ have also been revealed by the Raman scattering data where damping of the A-BO_3 mode was detected for $x \geqslant x_{MPB}$ [26]. With these characteristics, the composition-driven local structural phase transition may be categorized as an order-disorder type, which

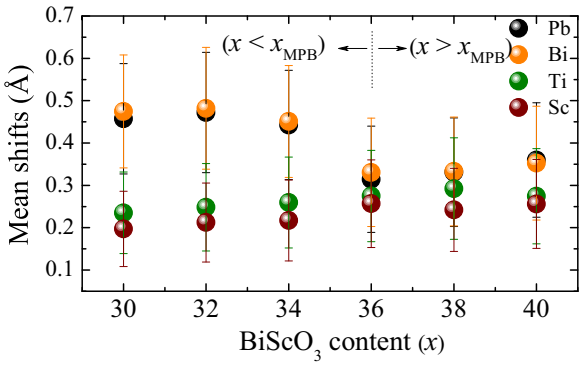

FIG. 4. Mean shifts of the cations along with their standard deviations as a function of composition.

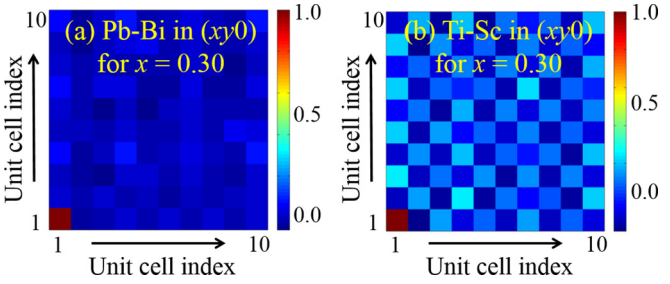

FIG. 5. Values of occupational pair-correlation function c_{ij} in the (xy0) plane, suggesting a B-site cation ordering.

could also be linked to the degeneracy of the average structural models to describe the MPB composition. For example, the recent reports [9,11] on driving the average symmetry of the compound at MPB from monoclinic to tetragonal by applying electric field or stress could essentially be interpreted as an alignment process of randomly oriented local polarizations in a relaxed state.

Figure 4 shows the mean shifts of the cations along with their standard deviations determined by fitting a normal distribution to the histogram of the actual shifts for different cations as a function of composition. It is evident that A-site cations have relatively larger displacements $\sim 0.31 - 0.48$ Å and sigmas $\sim 0.13 - 0.14$ Å than the B-site cations ($\sim 0.23 - 0.26$ Å and $\sim 0.09 - 0.12$ Å, respectively). Large shifts of Pb with respect to its oxygen environment is common for Pb-based perovskites [8,30–32], and this is often described as one of the main reasons for better ferroelectric properties of the Pb-based systems, which are typically termed as A-site active ferroelectric [33]. It is further interesting to see here that xBS $-$ PT is moving from strongly A-site driven ferroelectrics to competing A- and B-site ferroelectrics for $x \geqslant x_{\mathrm{MPB}}$.

In order to check for possible cation ordering or correlations either in occupancies or in displacements of different cations sitting at the same crystallographic site, we have calculated the following pair-correlation functions, respectively [34]:

$$c_{ij} = \frac{P_{ij} - \theta^2}{\theta(1-\theta)}, \quad d_{ij} = \frac{\langle x_i x_j \rangle}{\sqrt{\langle x_i^2 \rangle \langle x_j^2 \rangle}}, \tag{1}$$

where P_{ij} refers to the total probability of sites i and j being occupied by the same type of atom, θ is the concentration of the cation in the system, and x_i is the displacement of the atom on site i from its average position in a defined direction. Negative values of c_{ij} refer to the case where the two sites i and j tend to be occupied by different types of atoms, while positive values indicate that sites i and j tend to be occupied by the same type of atom. A correlation value of zero describes a random distribution. Likewise a positive value of d_{ij} corresponds to coupled displacements, while a negative value will indicate anticoupled displacements.

Figure 5 shows the values of c_{ij} in a plane (xy0) for $x = 0.30$. It is evident that Pb and Bi are completely random in terms of occupying the A site of the structure; however, there is a tendency of ordering between Ti and Sc at the B site [Fig. 6(b)]. For the rest of the pseudocubic directions and planes [($x0z$) and ($0yz$)] we obtained similar results for both groups. Although there is a little variance among the individual runs for a particular composition, the overall features remain the same. In addition, it is not conclusive if there is a specific trend for the values of c_{ij} of B-site cations as a function of composition. Further, the values of d_{ij} did not show any trend for either A- or B-site cations, suggesting the displacements are uncorrelated between Pb and Bi or Ti and Sc ions irrespective of the composition (see Supplemental Material [35]).

In summary, we have provided a picture showing the variation of microscopic polarization as a function of composition for xBS $-$ PT from which the MPB can be identified as a critical composition where the cations have demonstrated enhanced randomness in their shift directions. This provides a new perspective that can be referred to as a "model of randomness" in defining an MPB in a phase diagram of a Pb-based ferroelectric solid solution, exclusively based on the local structural information. This model has been conceived through RMC modeling of the neutron PDF data, which enabled us to extract distinct characteristics of the individual cation with varying composition. The features observed in the stereograms further imply that the inclusion of Bi and Sc in the system has initially affected the polarizations of the lighter B-site cations; however, there exists a critical fraction of the doping when the system experiences maximum structural instability characterized by the abrupt increase in the orientational disorder of the A-site cations at the MPB. Hence it emphasizes the critical role of the B-site disorder for promoting the much sought-after MPB properties in ferroelectric solid solutions [16]. Finally, we anticipate that similar investigations are required on a diverse range of systems including Pb-free systems in order to build a more general understanding of the MPB behavior, and thereby to establish the crucial structure-property connections.

Financial support from BMBF (Projects No. 05K10WEB and No. 05K13WE2) and Deutsche Forschungsgemeinschaft (MI No. 1127/8-1) are gratefully acknowledged. Parts of this research were carried out at PETRA III, DESY, a member of the Helmholtz Association of German Research Centres. We would like to thank Martin v. Zimmermann and J. Bednarcik for assistance in using beamline BW5 of DORIS facility. K.D. would like to thank Matt Tucker from ISIS, UK for many suggestions on using the RMCprofile package, and Boriana Mihailova from University of Hamburg for several useful discussions.

[1] R. Guo, L. E. Cross, S.-E. Park, B. Noheda, D. E. Cox, and G. Shirane, Phys. Rev. Lett. **84**, 5423 (2000).

[2] B. Noheda, D. E. Cox, G. Shirane, S. E. Park, L. E. Cross, and Z. Zhong, Phys. Rev. Lett. **86**, 3891 (2001).

[3] R. E. Eitel, C. A. Randall, T. R. Shrout, P. W. Rehrig, W. Hackenberger, and S. E. Park, Jpn. J. Appl. Phys. **40**, 5999 (2001).

[4] R. E. Eitel, C. A. Randall, T. R. Shrout, and S. E. Park, Jpn. J. Appl. Phys. **41**, 2099 (2002).

[5] R. E. Eitel, S. J. Zhang, T. R. Shrout, C. A. Randall, and I. Levin, J. Appl. Phys. **96**, 2828 (2004).

[6] J. Chaigneau, J. M. Kiat, C. Malibert, and C. Bogicevic, Phys. Rev. B **76**, 094111 (2007).

[7] K. Datta, D. Walker, and P. A. Thomas, Phys. Rev. B **82**, 144108 (2010).

[8] T. Egami, Annu. Rev. Mater. Res. **37**, 297 (2007).

[9] Lalitha K. V., A. N. Fitch, and R. Ranjan, Phys. Rev. B **87**, 064106 (2013).

[10] J. L. Jones, E. Aksel, G. Tutuncu, T. M. Usher, J. Chen, X. Xing, and A. J. Studer, Phys. Rev. B **86**, 024104 (2012).

[11] Lalitha K. V., A. K. Kalyani, and R. Ranjan, Phys. Rev. B **90**, 224107 (2014).

[12] D. J. Goossens, ISRN Mater. Sci. **2013**, 1 (2013).

[13] R. G. Burkovsky, Y. A. Bronwald, A. V. Filimonov, A. I. Rudskoy, D. Chernyshov, A. Bosak, J. Hlinka, X. Long, Z.-G. Ye, and S. B. Vakhrushev, Phys. Rev. Lett. **109**, 097603 (2012).

[14] A. M. George, J. Iñiguez, and L. Bellaiche, Phys. Rev. Lett. **91**, 045504 (2003).

[15] L. Bellaiche and A. M. George, Nature (London) **413**, 54 (2001).

[16] I. Grinberg, V. Cooper, and A. Rappe, Nature (London) **419**, 909 (2002).

[17] T. Egami and S. Billinge, *Underneath the Bragg Peaks Structural Analysis of Complex Materials* (Pergamon Materials Series, New York, 2012).

[18] R. L. McGreevy, J. Phys.: Condens. Matter **13**, R877 (2001).

[19] H. Y. Playford, L. R. Owen, I. Levin, and M. G. Tucker, Annu. Rev. Mater. Res. **44**, 429 (2014).

[20] N. Zhang, H. Yokota, A. M. Glazer, Z. Ren, D. A. Keen, D. S. Keeble, P. A. Thomas, and Z.-G. Ye, Nat. Commun. **5**, 5231 (2014).

[21] I.-K. Jeong, T. W. Darling, J. K. Lee, T. Proffen, R. H. Heffner, J. S. Park, K. S. Hong, W. Dmowski, and T. Egami, Phys. Rev. Lett. **94**, 147602 (2005).

[22] W. Dmowski, M. K. Akbas, P. K. Davies, and T. Egami, J. Phys. Chem. Solids **61**, 229 (2000).

[23] I.-K. Jeong, J. K. Lee, and R. H. Heffner, Appl. Phys. Lett. **92**, 172911 (2008).

[24] I.-K. Jeong, C. Y. Park, J. S. Ahn, S. Park, and D. J. Kim, Phys. Rev. B **81**, 214119 (2010).

[25] D. S. Keeble, E. R. Barney, D. A. Keen, M. G. Tucker, J. Kreisel, and P. A. Thomas, Adv. Funct. Mater. **23**, 185 (2013).

[26] K. Datta, A. Richter, M. Göbbels, R. B. Neder, and B. Mihailova, Phys. Rev. B **92**, 024107 (2015).

[27] M. G. Tucker, M. T. Dove, and D. A. Keen, J. Appl. Crystallogr. **34**, 630 (2001).

[28] T. Proffen and R. Neder, J. Appl. Crystallogr. **30**, 171 (1997).

[29] Y. Shimojo, R. Wang, T. Sekiya, T. Nakamura, and L. E. Cross, Ferroelectrics **284**, 121 (2003).

[30] T. Egami, S. Teslic, W. Dmowski, D. Viehland, and S. Vakhrushev, Ferroelectrics **199**, 103 (1997).

[31] T. Egami, W. Dmowski, M. Akbas, and P. K. Davies, in *Local Structure and Polarization in Pb Containing Ferroelectric Oxides*, AIP Conf. Proc. No. 436 (AIP, New York, 1998), p. 1.

[32] G. H. Kwei, S. J. L. Billinge, S.-W. Cheong, and J. G. Saxton, Ferroelectrics **164**, 57 (1995).

[33] M. Ghita, M. Fornari, D. J. Singh, and S. V. Halilov, Phys. Rev. B **72**, 054114 (2005).

[34] T. Proffen, V. Petkov, S. J. L. Billinge, and T. Vogt, Z. Kristallogr. **217**, 47 (2002).

[35] See Supplemental Material at http://link.aps.org/supplemental/10.1103/PhysRevB.93.064102 for additional figures.